NIH Public Access

Author Manuscript

Nanotechnology. Author manuscript; available in PMC 2011 January 1.

Published in final edited form as:

Nanotechnology. 2010 January 8; 21(1): 015705. doi:10.1088/0957-4484/21/1/015705.

Single-layer graphene on Al_2O_3/Si substrate: better contrast and higher performance of graphene transistors

Lei Liao[1], **Jingwei Bai**[2], **Yongquan Qu**[1], **Yu. Huang**[2,3,a)], and **Xiangfeng Duan**[1,3,a)]

[1] Department of Chemistry and Biochemistry, University of California, Los Angeles, California 90095, USA

[2] Department of Materials Science and Engineering, University of California, Los Angeles, California 90095, USA

[3] California Nanosystems Institute, University of California, Los Angeles, California 90095, USA

Abstract

The fact that single-layer graphene can be visualized on 300 nm SiO_2/Si substrate using optical microscope has enabled the facile fabrication of single-layer graphene devices for fundamental studies and potential applications. Here we report an Al_2O_3/Si substrate for the fabrication of graphene devices with better contrast and higher performance. Our studies show that the contrast of single-layer graphene on 72 nm Al_2O_3/Si substrate is much better than that of single-layer graphene on 300 nm SiO_2/Si substrate. Moreover, the transconductance of single-layer graphene transistors on Al_2O_3/Si substrate shows a more than 7-fold increase, due to the smaller dielectric thickness and higher dielectric constant in 72 nm Al_2O_3 film. These studies demonstrate a new and superior substrate for the fabrication of graphene transistors, and are of significance for both fundamental studies and technological applications.

Keywords

graphene; high-*k* dielectrics; contrast; field effect transistor

1. Introduction

Graphene is a one-atom-thick planar sheet of sp^2-bonded carbon atoms that are arranged in a honeycomb crystal lattice. As a gapless semiconductor, charge carriers in graphene can be tuned continuously from electrons to holes, crossing the charge neutral Dirac point using an external electric field [1–7]. Graphene-based electronics is currently the subject of intense focus for nanoscale electronic applications due to its exceptional electronic properties including carrier mobilities exceeding 100,000 $cm^2/V{\cdot}s$ and a micrometer-scale mean free path at room temperature [8–10].

Most efforts to date employ a silicon substrate as a global back gate and a 300 nm thick silicon dioxide (SiO_2) as the gate dielectric. This substrate is used primarily because the graphene can be readily visualized using optical microscope on this particular substrate due to optical interference [11–13]. The readily viewable graphene on the 300 nm SiO_2 substrate has allowed easy device fabrication and led to many interesting scientific discoveries. The requirement of 300 nm SiO_2, however, can intrinsically limit the resulted device performance in several

[a)] To whom correspondence should be addressed. xduan@chem.ucla.edu, yhuang@seas.ucla.edu.

NIH-PA Author Manuscript

NIH-PA Author Manuscript

NIH-PA Author Manuscript

NIH-PA Author Manuscript NIH-PA Author Manuscript NIH-PA Author Manuscript

perspectives. First, optical detection technique to visualize graphene has been demonstrated and widely used only for a SiO_2 thickness of 300 nm, but a 5% variation in thickness (e.g. to 315 nm) can significantly lower the contrast [11,14]. Second, the devices made on 300 nm SiO_2 substrate often have too small gate capacitance due to relatively large thickness and small dielectric constant, and thus require high switching voltage.

Recently, it has been predicted that the 72 nm Al_2O_3 film can be much better for visualizing graphene than SiO_2 and Si_3N_4 films by total color difference calculation [14,]. Moreover, Al_2O_3, with a dielectric constant of 9.1, is an important high-*k* materials with excellent dielectric properties, thermal and chemical stability [15]. Therefore, higher performance graphene transistors may be readily fabricated on 72 nm Al_2O_3/Si substrate. Here we report the integration of graphene on 72 nm Al_2O_3/Si substrate and investigation of the optical contrast and device performance. Compared to 300 nm SiO_2/Si substrate, 72 nm Al_2O_3/Si substrate could enhance the normalized optical contrast of single-layer graphene (SLG) by approximately 3 times. Furthermore, higher performance of graphene transistors can be achieved on 72 nm Al_2O_3/Si substrate with over 7-fold increase in transconductance.

2. Experimental

Al_2O_3 film was deposited on top of heavily-doped *p*-type silicon (100) wafers by an atomic layer deposition (ALD) technique at 250 °C using trimethylaluminum and distilled water as the source. Prior to the deposition of the Al_2O_3 layer, the native oxide layer on the Si wafer was removed with buffered oxide etching. After 72 nm Al_2O_3 film was deposited, graphene layers were mechanically peeled onto the substrate. As a control, graphene was also peeled onto standard 300 nm SiO_2/Si wafers. The substrates are then calcined at 300 °C to remove organic residue. The morphologies of the samples were characterized by atomic force microscope (AFM, Veeco Dimension 5000) and optical microscope (Olympus), respectively. The Raman spectra were recorded by a Renishaw inVia Raman spectroscopy. The thickness and refractive index of Al_2O_3 film were obtained by Sopra GES5 Ellipsometer.

Metal-insulator-semiconductor (MIS) devices were used to investigate the dielectric properties of the Al_2O_3 film. The MIS devices were made on Al_2O_3/Si substrate with circular electrodes of 100 μm in diameter, fabricated using e-beam lithography followed by e-beam metal (Ti/Au, 50/50 nm) deposition. The SLG field-effect transistors (FETs) were also fabricated by the standard e-beam lithography and e-beam evaporation (Ti/Au, 50/50 nm) process. The on-off ratio of SLG FETs is usually very low because the intrinsic SLG is a semimetal with zero band-gap. It has been demonstrated that a band gap can open up by fabricating graphene nanostructures of confined geometry such as graphene nanoribbons (GNRs)[16–21]. To this end, we have also fabricated GNR FETs on Al_2O_3/Si substrate with a recently reported procedure using chemically defined nanowires as the nanoscale etching mask [19]. The electrical transport properties were measured by a Lakeshore probe station with a home built data acquisition system. Capacitance vs voltage (C-V) measurements were performed using a Stanford Research Systems SR720 LCR Meter.

3. Results and Discussion

An AFM image of Al_2O_3 film on Si substrate indicates that the root mean square roughness for Al_2O_3 on Si substrate is less than 0.5 nm (Fig. 1a). To understand the dielectric properties of the Al_2O_3 film, metal-insulator-semiconductor (MIS) devices were used to characterize the capacitance-voltage, current tunneling and breakdown characteristics. The C-V plot for the 72 nm Al_2O_3 film (Figure 1b) shows an accumulation of charges in the silicon substrate in negative polarity and a depletion of charges in the positive polarity, consistent with p-type substrate used. The dielectric constant can then be calculated using: $\varepsilon = Cd/\varepsilon_0 A$, where C is the insulate

NIH-PA Author Manuscript

capacitance (highest capacitance in the C-V curve), d is thickness of the film, ε_0 is the permittivity of free space, and A is the area. The obtained dielectric constant is 7.5, consistent with previous reports on ALD Al_2O_3 films [15]. Current-voltage (I-V) measurements of the MIS device show typical Fowler–Nordheim (F-N) tunneling behaviour with a breakdown field of 6.7 MV/cm (Fig. 1c and 1d), comparable to the best quality ALD Al_2O_3 films [15]. This type of field assisted tunneling can be described by charge carriers tunneling through a triangular barrier with [15]:

$$J=AE_{OX}^{2}\exp(-B/E_{OX}) \quad (1)$$

where

$$A=1.54\times10^{-6}\left\{\frac{1}{m^{*}\Phi_{B}}\right\} \quad (2)$$

and

$$B=6.83\times10^{7}(m^{*})^{1/2}(\Phi_{B})^{3/2} \quad (3)$$

J is current density, E_{ox} is the oxide electric field, m^* is the effective mass of the charge carrier, which is about 0.23, and Φ_B is the barrier height. Fitting the I-V characteristics with F-N tunnelling model gives a tunnel barrier of about 2.2 eV between Al_2O_3 and Ti, comparable to previous reports of the barrier height between ALD Al_2O_3 and metals of similar work function [15,22]. These studies clearly demonstrate that the quality of our Al_2O_3 film is good enough as high-k gate dielectrics [15].

Next we discuss the optical contrast of SLG on Al_2O_3 films. Optical contrast is the difference in visual properties that enable us to distinguish an object from other objects and the background. Remarkably, when a proper substrate is used, single layer or few layers of graphene can be observed with sufficient contrast using an normal optical microscope [23]. The origin of the contrast can be explained by Fresnel's equations [11]. Figure 2a and 2b show the optical image of SLG samples on Al_2O_3/Si and SiO_2/Si substrate. The relative Raman spectra prove that samples are perfect SLG (Figure 2e). Importantly, the SLG on Al_2O_3/Si is much better visualized than that on SiO_2/Si substrate. To quantify the difference in the contrast of the SLG samples on Al_2O_3/Si and SiO_2/Si substrates, the color images are converted to gray-scale images with same normalized background intensity shown in Figure 2c and 2d. Indeed, the contrast intensity of SLG on Al_2O_3/Si is significantly stronger than that of SLG on SiO_2/Si. The Weber contrast C(λ) is defined as $C(\lambda) = (R_0(\lambda)-R(\lambda))/R_0(\lambda)$ [11,23], where $R_0(\lambda)$ is the reflected light intensity of background and R(λ) is the reflected light intensity from graphene sheet. The contrast of SLG on Al_2O_3/Si is 0.070, which is 3 times larger than that of SLG on SiO_2/Si with 0.023 in our system (Figure 2c and 2d). Considering the incident light from air (n = 1) onto a graphene, SiO_2 or Al_2O_3, and Si trilayer system, the reflected light intensity from the trilayer system can be described by [11,23]:

$$R(\lambda)=r(\lambda)r^{*}(\lambda) \quad (4)$$

NIH-PA Author Manuscript

NIH-PA Author Manuscript

NIH-PA Author Manuscript

$$r(\lambda)=\frac{r_a}{r_b} \quad (5)$$

$$r_a=(r_1e^{i(\beta_1+\beta_2)}+r_2e^{-i(\beta_1-\beta_2)}+r_3e^{-i(\beta_1+\beta_2)}+r_1r_2r_3e^{i(\beta_1-\beta_2)}) \quad (6)$$

$$r_b=(e^{i(\beta_1+\beta_2)}+r_1r_2e^{-i(\beta_1-\beta_2)}+r_1r_3e^{-i(\beta_1+\beta_2)}+r_1r_2r_3e^{i(\beta_1-\beta_2)}) \quad (7)$$

where $r_1 = (n_0-n_1)/(n_0+n_1)$, $r_2 = (n_1-n_2)/(n_1+n_2)$, and $r_3 = (n_2-n_3)/(n_2+n_3)$ are the reflection coefficients for different interfaces and $\beta_1 = 2\pi n_1(d_1/\lambda)$ and $\beta_2 = 2\pi n_2(d_2/\lambda)$ are the phase differences when light passes through the media which is determined by the path difference of two neighboring interfering light beams. The calculated contrast spectra of SLG are shown in Figure 2f. The best contrast of graphene on Al_2O_3/Si could be obtained with 450 nm light illumination. Moreover, there is moderate contrast intensity in whole visible light wavelength, in contrast to the SiO_2/Si system where relatively strong contrast is only observed in the red region.

The excellent dielectric properties observed in Al_2O_3 film and the better optical contrast of SLG on Al_2O_3 film readily allows us to fabricate graphene transistors on Al_2O_3/Si substrate. To compare with previous studies, we adopted a similar back gated structure where Al_2O_3 is used the gate dielectrics and Si substrate used as the back gate. Similar devices are also fabricated on the standard SiO_2/Si substrate as a control. A schematic device diagram and an SEM image of the graphene FET are shown in Figure 3a. To evaluate and compare the device performance for devices based on SiO_2 and Al_2O_3, we have measured the transfer characteristics (Drain-source current I_{ds} versus gate voltage V_g). The normalized transconductance $g_m=\frac{dI_{ds}}{dV_g}\cdot\frac{L}{W}$ can be extracted from the linear region of the $I_{ds}-V_g$ curve. Significantly, the $I_{ds}-V_g$ data show a significant improvement in transconductance when the Al_2O_3 is used (Fig. 3b). Figure 3c shows the measured normalized transconductance of the SLG FET as a function of gate voltage V_g. At V_{ds} = 0.1V, the Al_2O_3 bottom-gated device exhibits a g_m of about 22.1 μS, which is around 7 times larger than that of the SiO_2 back-gated device (g_m ~ 3.1 μS). This substantial improvement can be attributed to a much stronger gate coupling due to smaller thickness and higher dielectric constant material used in the this devices (72 nm Al_2O_3 with k = 7.5 *vs.* 300 nm SiO_2 with k = 3.9). In order to evaluate the mobility of the devices, a device model was used [24, 25]. The extracted carrier mobility of SLG FET on Al_2O_3 is 7400 $cm^2/V\cdot s$, which is similar to 8200 $cm^2/V\cdot s$ of the FET on SiO_2.

To further increase the on-off ratio of the device, we have also fabricated GNR devices on Al_2O_3/Si substrate and studied the device performance. Here a SiO_2 nanowire was used as a nanoscale etch mask to define a graphene nanoribbon with a width in the 10–20 nm regime and the schematic device diagram of the GNR FET is shown in Figure 4a. The Figure 4b plots the $I_{ds}-V_{ds}$ of the top-gated device under various gate voltages (V_g) of −8, −6, −4, −2, 0, and 2V. It shows clearly that the conductance of the nanoribbon decreases as the gate potential increases, demonstrating that the graphene nanoribbon is *p*-type doped, which can be attributed to edge oxidation or the physisorbed O_2 from ambient or during the device fabrication process. Transfer characteristics show the GNR transistor on Al_2O_3 dielectric can be switched on and off with approximately 6 volts of gate swing (Fig. 4c), in contrast to ~30 V required for SiO_2 back gated devices (inset, Fig. 4c) and 10–40 V for previously reported devices on SiO_2 [18–

NIH-PA Author Manuscript

20], and the transconductance g_m of about 3.2 μS, also more than 9 time larger than that of the back-gated GNR transistor on SiO_2/Si (~0.36 μS) (Fig. 4c). The device shows a room temperature on/off ratio of ~10 at V_{ds} = 0.1 V, which is consistent with a graphene nanoribbon with an estimated width of 10–15 nm.

4. Conclusions

In summary, we have demonstrated that 72 nm Al_2O_3/Si substrate can be a superior substrate to 300 nm SiO_2/Si substrate for the visualization of graphene and fabrication of graphene transistors. Compared to 300 nm SiO_2/Si substrate, 72 nm Al_2O_3/Si substrate could enhance the optical contrast of SLG by at least 3 times. Furthermore, using the Al_2O_3 film as the gate dielectrics, the back-gated graphene FETs have been fabricated to exhibit more than 7-fold increase in transconductance. This study demonstrates a new and superior substrate for the fabrication of graphene transistors, and is of significance for both fundamental studies and technological applications.

Acknowledgments

We acknowledge Nanoelectronics Research Facility at UCLA for support of device fabrication. Y.H. acknowledges support from the Henry Samueli School of Engineering and an Applied Science Fellowship. X.D. acknowledges support by the NIH Director's New Innovator Award Program, part of the NIH Roadmap for Medical Research, through grant number 1DP2OD004342-01. L.L. acknowledges the discussion with YingYing Wang in Nanyang Technological University for the calculation of the contrast.

References

1. Geim AK, Novoselov KS. Nature Materials 2007;6:183.
2. Geim AK. Science 2009;324:1530. [PubMed: 19541989]
3. Novoselov KS, Geim AK, Morozov SV, Jiang D, Zhang Y, Dubonos SV, Grigorieva IV, Firsov AA. Science 2004;306:666. [PubMed: 15499015]
4. Bunch JS, Yaish Y, Brink M, Bolotin K, McEuen PL. Nano Letters 2005;5:287. [PubMed: 15794612]
5. Novoselov KS, Geim AK, Morozov SV, Jiang D, Katsnelson MI, Grigorieva IV, Dubonos SV, Firsov AA. Nature 2005;438:197. [PubMed: 16281030]
6. Zhang YB, TanY W, Stormer H, Land Kim P. Nature 2005;438:201. [PubMed: 16281031]
7. Berger C, Song ZM, Li XB, Wu XS, Brown N, Naud C, Mayou D, Li TB, Hass J, Marchenkov AN, Conrad EH, First PN, de Heer WA. Science 2006;312:1191. [PubMed: 16614173]
8. Avouris P, Chen ZH, Perebeinos V. Nature Nanotechnology 2007;2:605.
9. Lemme MC, Echtermeyer TJ, Baus M, Kurz H. IEEE Electron Device Letters 2007;28:282.
10. Lin YM, Jenkins KA, Valdes-Garcia A, Small JP, Farmer DB, Avouris P. Nano Letters 2009;9:422. [PubMed: 19099364]
11. Blake P, Hill EW, Neto AHC, Novoselov KS, Jiang D, Yang R, Booth TJ, Geim AK. Applied Physics Letters 2007;91:063124.
12. Jung I, Pelton M, Piner R, Dikin DA, Stankovich S, Watcharotone S, Hausner M, Ruoff RS. Nano Letters 2007;7:3569.
13. Abergel DSL, Russell A, Fal'ko VI. Applied Physics Letters 2007;91:063125.
14. Gao LB, Ren WC, Li F, Cheng HM. ACS Nano 2008;2:1625. [PubMed: 19206365]
15. Groner, MD.; Elam, JW.; Fabreguette, FH.; George, SM. Thin Solid Films. Vol. 413. 2002. p. 186
16. Chen, ZH.; Lin, YM.; Rooks, MJ.; Avouris, P. Physica E. Vol. 40. 2007. p. 228
17. Han, MY.; Ozyilmaz, B.; Zhang, YB.; Kim, P. Physical Review Letters. 2007. p. 98
18. Li, XL.; Wang, XR.; Zhang, L.; Lee, SW.; Dai, HJ. Science. Vol. 319. 2008. p. 1229
19. Bai, JW.; Duan, XF.; Huang, Y. Nano Letters. Vol. 9. 2009. p. 2083
20. Jiao, LY.; Zhang, L.; Wang, XR.; Diankov, G.; Dai, HJ. Nature. Vol. 458. 2009. p. 877

NIH-PA Author Manuscript
NIH-PA Author Manuscript
NIH-PA Author Manuscript

21. Kosynkin DV, Higginbotham AL, Sinitskii A, Lomeda JR, Dimiev A, Price BK, Tour JM. Nature 2009;458:872. [PubMed: 19370030]
22. Afanas'ev VV, Houssa M, Stesmans A, Adriaenssens GJ, Heyns MM. J Non-Cryst Solids 2002;303:69.
23. Ni ZH, Wang HM, Kasim J, Fan HM, Yu T, Wu YH, Feng YP, Shen ZX. Nano Letters 2007;7:2758. [PubMed: 17655269]
24. Kim S, Nah J, Jo I, Shahrjerdi D, Colombo L, Yao Z, Tutuc E, Banerjee SK. Applied Physics Letters 2009;94:062107.
25. Meric I, Han MY, Young AF, Ozyilmaz B, Kim P, Shepard KL. Nature Nanotechnology 2008;3:654.

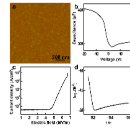

Figure 1.
(a) AFM image of Al_2O_3 film by ALD. (b) Capacitance vs voltage (C-V) curve of an MIS device with 72 nm Al_2O_3 film on Si substrate. (c) Current-voltage (I-V) curve of the MIS device made from Al_2O_3 film, and (d) the corresponding Fowler–Nordheim (F-N) curve.

NIH-PA Author Manuscript
NIH-PA Author Manuscript
NIH-PA Author Manuscript

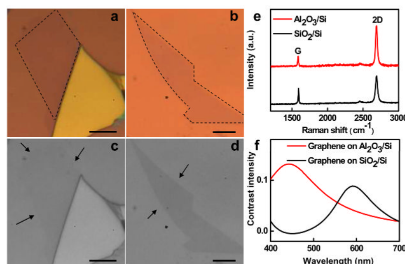

Figure 2.

(a) and (b) Optical image of graphene on 300 nm SiO_2/Si and 72 nm Al_2O_3/Si substrate. The dashed lines highlight the edge of the single layer graphene region. (c) and (d) the gray-scale optical image from (a) and (b). The arrows highlight the edge of the single layer graphene region. (e) Raman spectra of the single-layer graphene on 300 nm SiO_2/Si and 72 nm Al_2O_3/Si substrates. (f) The contrast spectra of single-layer graphene 300 nm SiO_2/Si and 72 nm Al_2O_3/Si substrates.

NIH-PA Author Manuscript
NIH-PA Author Manuscript
NIH-PA Author Manuscript

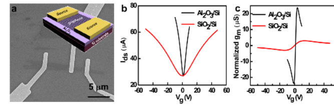

Figure 3.

(a) SEM image of a graphene field-effect transistor on a 72-nm Al_2O_3/Si substrate, and the inset shows schematics of the device. (b) $I_{ds}-V_g$ curves of graphene FET on 300 nm SiO_2/Si and 72 nm Al_2O_3/Si substrate, (c) g_m-V_g curves of graphene FET on 300 nm SiO_2/Si and 72 nm Al_2O_3/Si substrate.

NIH-PA Author Manuscript

NIH-PA Author Manuscript

NIH-PA Author Manuscript

NIH-PA Author Manuscript

NIH-PA Author Manuscript

NIH-PA Author Manuscript

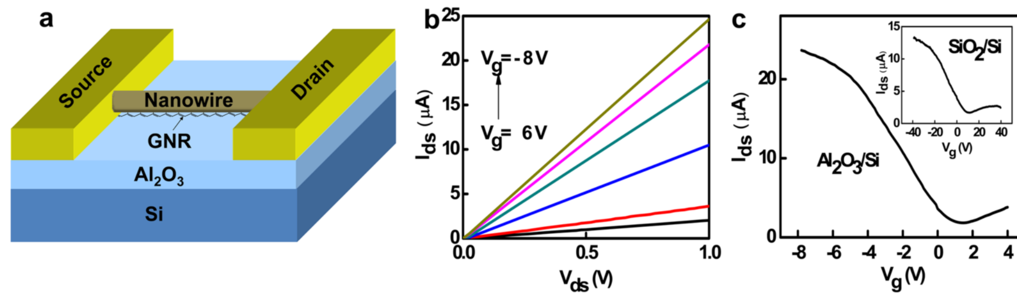

Figure 4.
(a) The schematics of the GNR FET device. (b) $I_{ds}-V_{ds}$ curves of a GNR-FET on 72 nm Al_2O_3/Si substrate. (c) $I_{ds}-V_g$ curves of the GNR-FETs on the 72nm Al_2O_3/Si substrate and the 300 nm SiO_2/Si substrate (inset).